Synthesis of the Salts $[N(PPh_3)_2]_2[M(CO)_3(\eta^6\text{-}7,9\text{-}Me_2\text{-}7,9\text{-}C_2B_{10}H_{10})]$[†] (M = Mo or W) and Their Use as Reagents for Preparing Polynuclear Metallacarborane Cluster Compounds

Nicholas Carr, Donald F. Mullica, Eric L. Sappenfield, F. Gordon A. Stone,* and Michael J. Went

Department of Chemistry, Baylor University, Waco, Texas 76798-7348

Received June 22, 1993[®]

Treatment of the compounds $[M(CO)_3(NCEt)_3]$ (M = Mo or W) with $Na_2[\textit{nido}\text{-}7,9\text{-}Me_2\text{-}7,9\text{-}C_2B_{10}H_{10}]$ in thf (tetrahydrofuran) affords the complex anions $[M(CO)_3(\eta^6\text{-}7,9\text{-}Me_2\text{-}7,9\text{-}C_2B_{10}H_{10})]^{2-}$ which have been isolated as their $[N(PPh_3)_2]^+$ salts [**2a**, M = Mo; **2b**, M = W]. Reactions of these reagents with *cis*-$[PtCl_2(CO)(PPh_3)]$ in thf, in the presence of $TlPF_6$, yield separable mixtures of the di- and trinuclear metal species $[MPt(CO)_4(PPh_3)(\eta^6\text{-}7,9\text{-}Me_2\text{-}7,9\text{-}C_2B_{10}H_{10})]$ [**4c**, M = Mo; **4d**, M = W] and $[MPt_2(\mu\text{-}CO)(CO)_3(PPh_3)_2(\eta^6\text{-}7,9\text{-}Me_2\text{-}7,9\text{-}C_2B_{10}H_{10})]$ [**8a**, M = Mo; **8b**, M = W], respectively. The structure of compound **8a** has been established by X-ray diffraction. Crystals are monoclinic, space group $P2_1/n$ (No. 14) with a = 13.047(2) Å, b = 13.856(2) Å, c = 27.103(6) Å, β = 102.13(2)°, and Z = 4. The core of the molecule consists of a triangle of metal atoms [Mo—Pt 2.707(1) and 2.950(1) Å, Pt—Pt 2.747(1) Å] with the molybdenum atom ligated by a $7,9\text{-}Me_2\text{-}7,9\text{-}C_2B_{10}H_{10}$ carborane cage, bound in the normal hexahapto manner, and one terminal carbonyl group. One of the Mo—Pt vectors is semibridged by two CO groups. Each platinum atom carries a PPh_3 ligand and the Pt—Pt vector is bridged essentially symmetrically by a carbonyl group [Pt—CO 1.996(8) and 2.026(7) Å]. In addition, the BH bond which is in a site β to the carbon atoms of the $\overline{\mathrm{CBCB}\mathit{B}\mathrm{B}}$ hexagonal ring of the carborane ligand is involved in an exopolyhedral three-center, two-electron B—H→Pt interaction. Treatment of the salts **2** with $[PtCl_2(cod)]$ (cod = cycloocta-1,5-diene) in the presence of $TlPF_6$ gives the trimetal compounds $[MPt_2(\mu\text{-}CO)(\mu_3\text{-}\sigma,\sigma'{:}\eta^6\text{-}7,9\text{-}Me_2\text{-}7,9\text{-}C_2B_{10}H_8)(CO)_2(cod)_2]$ [**7a**, M = Mo; **7b**, M = W] containing two exopolyhedral B—Pt σ-bonds. The cod ligands present in **7a** may be displaced by $[W(\equiv CC_6H_4Me\text{-}4)(CO)_2(\eta^5\text{-}C_5H_5)]$ to afford the pentanuclear complex $[MoW_2Pt_2(\mu\text{-}CC_6H_4Me\text{-}4)(\mu_3\text{-}CC_6H_4Me\text{-}4)(\mu_3\text{-}\sigma{:}\eta^6\text{-}7,9\text{-}Me_2\text{-}7,9\text{-}C_2B_{10}H_8\text{-}12\text{-}OC)(CO)_7\text{-}(\eta^5\text{-}C_5H_5)_2]$ (**9**). A single-crystal X-ray diffraction analysis of **9** has been carried out. Crystals are orthorhombic, space group *Pbcn* (No. 60) with a = 29.736(4) Å, b = 18.077(1) Å, c = 18.100(2) Å, and Z = 8. The molecular structure of **9** consists of an almost planar chain of MoPtWPtW atoms with both an edge-bridging [μ-C—W 1.79(4) Å, μ-C—Pt 1.93(4) Å] and a triply-bridging [μ-C—W 1.99(4) Å, μ-C—Pt 2.05(4) and 2.20(4) Å] tolylmethylidyne ligand. A novel feature of the structure is the presence of a CO group bridging one of the W—Pt bonds and also attached through its oxygen atom to the boron atom that is in a site α to the carbon atoms of the $\overline{\mathrm{CBC}\mathit{B}\mathrm{BB}}$ ring of the carborane ligand that is η^6-coordinated to the Mo atom. In addition, the β boron atom of this ring, $\overline{\mathrm{CBCB}\mathit{B}\mathrm{B}}$, forms an exopolyhedral B—Pt σ-bond to the same platinum atom that is involved in the $\mathrm{BO}\overline{\mathrm{C{—}Pt{—}W}}$ interaction. Upon treatment with PMe_3, the terminal $[W(\equiv CC_6H_4Me\text{-}4)(CO)_2(\eta^5\text{-}C_5H_5)]$ molecule present in **9** is displaced to yield the tetranuclear metal complex $[MoWPt_2(\mu_3\text{-}CC_6H_4Me\text{-}4)(\mu_3\text{-}\sigma{:}\eta^6\text{-}7,9\text{-}Me_2\text{-}7,9\text{-}C_2B_{10}H_8\text{-}12\text{-}OC)(CO)_5(PMe_3)_2(\eta^5\text{-}C_5H_5)]$ (**10**). The new metallacarborane cluster compounds have been characterized by IR and NMR spectroscopy, in addition to the X-ray diffraction studies.

Introduction

We have recently begun to explore the synthetic utility of salts of the dianionic species $[M(CO)_3(\eta^5\text{-}7,8\text{-}R_2\text{-}7,8\text{-}C_2B_9H_9)]^{2-}$ (R = H or Me) and $[M(CO)_3(\eta^6\text{-}7,9\text{-}Me_2\text{-}7,9\text{-}C_2B_{10}H_{10})]^{2-}$ (M = Mo or W) as precursors to compounds containing heteronuclear metal–metal bonds. Thus reactions of the thallium salts $Tl_2[M(CO)_3(\eta^5\text{-}7,8\text{-}Me_2\text{-}7,8\text{-}C_2B_9H_9)]$ (**1**), generated in situ from $[M(CO)_3(NCMe)_3]$ and $Tl[Tl\text{-}7,8\text{-}Me_2\text{-}7,8\text{-}C_2B_9H_9]$, with the platinum compound $[PtCl_2(PPh_3)_2]$ afford dinuclear metal complexes of formulation $[MPt(CO)_3(PPh_3)_2(\eta^5\text{-}7,8\text{-}Me_2\text{-}7,8\text{-}C_2B_9H_9)]$ (**3**).[1] NMR studies revealed that the tungsten complex exists as a mixture of two isomers (ca. 1:1), one of which, **3a**, has an exopolyhedral B–H→Pt three-center, two-

---

* To whom correspondence should be addressed.

[†] In the compounds described in this paper $[\textit{nido}\text{-}7,9\text{-}Me_2\text{-}7,9\text{-}C_2B_{10}H_{10}]^{2-}$ anions form *closo*-1,6-dicarba-4-metallacarborane structures. Use of this numbering scheme, however, results in a complex and confusing nomenclature for the polynuclear metal complexes reported herein. We have therefore chosen to treat the cages as *nido*-12 vertex ligands with numbering as for a docosahedron from which one vertex has been removed.

[®] Abstract published in *Advance ACS Abstracts,* October 1, 1993.

[1] Dossett, S. J.; Mullica, D. F.; Sappenfield, E. L.; Stone, F. G. A.; Went, M. J. *J. Chem. Soc., Dalton Trans.* 1993, 281.

0276-7333/93/2312-4350$04.00/0

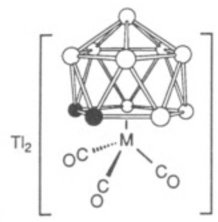

M
1a Mo
1b W

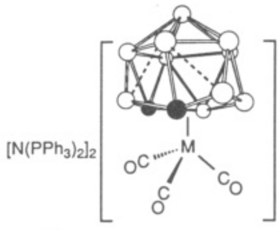

M
2a Mo
2b W

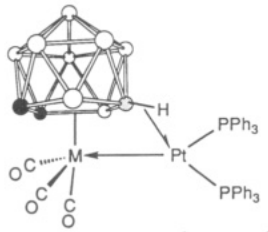

3a

M = Mo or W

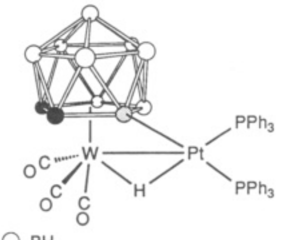

3b

electron interaction while the other has a B–Pt σ-bond and a bridging hydride ligand, [WPt(μ-H)(μ-σ:η^5-7,8-Me$_2$-7,8-C$_2$B$_9$H$_8$)(CO)$_3$(PPh$_3$)$_2$] (**3b**), resulting from oxidatively adding the BHPt group to the platinum center. Employing the sodium salts of [M(CO)$_3$(η^6-7,9-Me$_2$-7,9-C$_2$B$_{10}$H$_{10}$)]$^{2-}$ in similar reactions gives the related species [MPt(CO)$_3$(PPh$_3$)$_2$(η^6-7,9-Me$_2$-7,9-C$_2$B$_{10}$H$_{10}$)] (**4a, 4b**), containing the 13-vertex, 4,1,6-MC$_2$B$_{10}$ cage framework. Like compound **3** (M = W), these complexes are also formed as a mixture of two isomers, but interestingly the species structurally akin to **3a** with a B–H⇀Pt interaction are strongly favored for the 13-vertex metallacarborane species **4**. Related to these reactions, we have also observed that when the sodium salts of [M(CO)$_3$(η^5-7,8-R$_2$-7,8-C$_2$B$_9$H$_9$)]$^{2-}$ are treated with 2 equiv of [Rh(NCMe)$_3$(η^5-C$_5$Me$_5$)][BF$_4$]$_2$, the cluster compounds [MRh$_2$(μ-H)(μ-σ:η^5-7,8-R$_2$-7,8-C$_2$B$_9$H$_8$)(CO)$_3$(η^5-C$_5$Me$_5$)$_2$] (**5**) are formed in low yield (ca. 20%), along with the Rh(I) complex [Rh(CO)$_2$(η^5-C$_5$Me$_5$)]. In solution, some of these compounds also exist as an isomeric mixture, the second isomer containing two Rh–B σ-bonds and two bridging hydride ligands.[2]

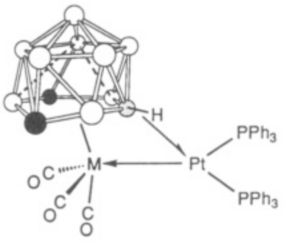

M
4a Mo
4b W

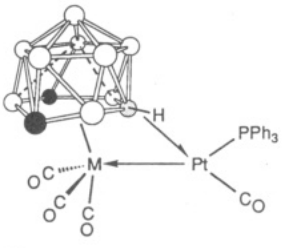

M
4c Mo
4d W

During the course of the earlier work,[1] it was observed that reaction of the sodium salts of [M(CO)$_3$(η^6-7,9-Me$_2$-7,9-C$_2$B$_{10}$H$_{10}$)]$^{2-}$ with [PtCl$_2$(cod)] (cod = cycloocta-1,5-diene) followed by addition of 2 equiv of PPh$_3$, did not give the neutral species **4a** and **4b**, as was expected, but rather afforded the salts [PtH(PPh$_3$)$_3$][MPt(μ-σ:η^6-7,9-Me$_2$-7,9-C$_2$B$_{10}$H$_9$)(CO)$_4$(PPh$_3$)] (**6**). Interestingly, protonation (HBF·Et$_2$O) of the latter gives the compounds

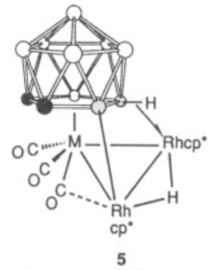

5

M = Mo or W
cp* = η^5-C$_5$Me$_5$

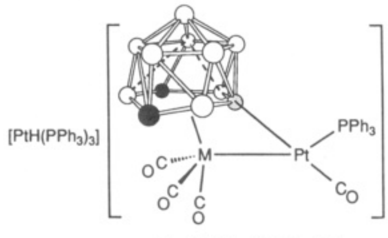

6

M = Mo or W

[MPt(CO)$_4$(PPh$_3$)(η^6-7,9-Me$_2$-7,9-C$_2$B$_{10}$H$_{10}$)] (**4c, 4d**), discussed further below. The synthesis of compounds **6** possibly suggests initial formation of a MPt$_2$ trinuclear metal species in which a cage BH bond has oxidatively added to one of the platinum centers to give a B–Pt σ-bond and a platinum hydride group. This trimetal intermediate could then be cleaved by phosphine to give the observed salts **6** having the [PtH(PPh$_3$)$_3$]$^+$ cation associated with the metal anion. This result and other related reactions of the salts of **2** with halide-containing platinum species are addressed in more detail in the work presented herein.

Results and Discussion

We have previously generated the salts Na$_2$[M(CO)$_3$(η^6-7,9-Me$_2$-7,9-C$_2$B$_{10}$H$_{10}$)] by treating the compounds [M(CO)$_3$(NCMe)$_3$] (M = Mo or W) with a thf (tetrahydrofuran) solution of Na$_2$[*nido*-7,9-Me$_2$-7,9-C$_2$B$_{10}$H$_{10}$], generated *in situ* by reducing C$_2$B$_{10}$H$_{10}$Me$_2$ in thf with sodium dihydronaphthylide,[3] and used these solutions without purification in subsequent reactions.[1] Although this methodology has proved reasonably successful, it does result in the formation of undesirable side products and hence in reduced yields of reaction products. We therefore undertook the isolation of the dianions with a suitable organic cation. This was readily achieved by addition of [N(PPh$_3$)$_2$]Cl to solutions of the sodium salts (generated as described above) and "workup" of the reaction mixtures to afford the relatively stable compounds [N(PPh$_3$)$_2$]$_2$[M(CO)$_3$(η^6-7,9-Me$_2$-7,9-C$_2$B$_{10}$H$_{10}$)] (**2a**, M = Mo; **2b**, M = W). Data characterizing these species are given in Tables I–III and are entirely as expected, except that the fluxionality associated with the carborane cage persists even at 190 K.

Treatment of the salts **2** with 1 mol equiv of [PtCl$_2$(cod)] in thf in the presence of TlPF$_6$, to facilitate removal of chloride ions as insoluble TlCl, affords the trinuclear compounds [MPt$_2$(μ-CO)(μ_3-σ,σ':η^6-7,9-Me$_2$-7,9-C$_2$B$_{10}$H$_8$)(CO)$_2$(cod)$_2$] (**7a**, M = Mo; **7b**, M = W). It is noteworthy that employing a "M:Pt:Tl" mole ratio of 1:2:4 gave no significant improvement in the yields of the species **7**. The presence of two B–Pt σ-bonds in these complexes is

---

[2] Mullica, D. F.; Sappenfield, E. L.; Stone, F. G. A.; Woollam, S. F. *J. Chem. Soc., Dalton Trans.*, in press.

[3] Dustin, D. F.; Dunks, G. B.; Hawthorne, M. F., *J. Am. Chem. Soc.* **1973**, *95*, 1109.

Table I. Physical and Infrared Absorption Data

compd	color	yield (%)	ν_{max}(CO)[a]/cm^{-1}	analysis (%)[b] C	analysis (%)[b] H
2a, $[N(PPh_3)_2]_2[Mo(CO)_3(\eta^6\text{-}7,9\text{-}Me_2\text{-}7,9\text{-}C_2B_{10}H_{10})]$	yellow	83	1895 (s), 1793 (m), 1778 (m)	65.30 (66.38)[c]	5.23 (5.36)
2b, $[N(PPh_3)_2]_2[W(CO)_3(\eta^6\text{-}7,9\text{-}Me_2\text{-}7,9\text{-}C_2B_{10}H_{10})]$	orange	81	1890 (s), 1790 (m), 1772 (m)	61.62 (62.54)[d]	4.74 (5.05)
7a, $[MoPt_2(\mu\text{-}CO)(\mu_3\text{-}\sigma,\sigma'\text{:}\eta^6\text{-}7,9\text{-}Me_2\text{-}7,9\text{-}C_2B_{10}H_8)\text{-}(CO)_2(cod)_2]$	orange	48	1997 (s), 1940 (m), 1762 (m br)	29.03 (28.87)	4.15 (4.00)
7b, $[WPt_2(\mu\text{-}CO)(\mu_3\text{-}\sigma,\sigma'\text{:}\eta^6\text{-}7,9\text{-}Me_2\text{-}7,9\text{-}C_2B_{10}H_8)\text{-}(CO)_2(cod)_2]$	orange	40	1991 (s), 1934 (m), 1762 (m br)	27.02 (26.44)	3.76 (3.67)
8a, $[MoPt_2(\mu\text{-}CO)(CO)_3(PPh_3)_2(\eta^6\text{-}7,9\text{-}Me_2\text{-}7,9\text{-}C_2B_{10}H_{10})]$	red	48	2006 (s), 1904 (sh), 1874 (s), 1802 (m)	40.62 (40.81)	3.52 (3.58)
8b, $[WPt_2(\mu\text{-}CO)(CO)_3(PPh_3)_2(\eta^6\text{-}7,9\text{-}Me_2\text{-}7,9\text{-}C_2B_{10}H_{10})]$	red	34	1997 (s), 1912 (w), 1872 (s), 1806 (m)	38.04 (38.21)	3.31 (3.35)
9, $[MoW_2Pt_2(\mu\text{-}CC_6H_4Me\text{-}4)(\mu_3\text{-}CC_6H_4Me\text{-}4)(\mu_3\text{-}\sigma\text{:}\eta^6\text{-}7,9\text{-}Me_2\text{-}7,9\text{-}C_2B_{10}H_8\text{-}12\text{-}OC)(CO)_7(\eta^5\text{-}C_5H_5)_2]$	purple	26	2091 (m), 2012 (m), 2003 (s), 1974 (m), 1954 (w), 1936 (w), 1924 (m), 1896 (br), 1849 (br)[e]	29.96 (28.80)	2.54 (2.42)
10, $[MoWPt_2(\mu_3\text{-}CC_6H_4Me\text{-}4)(\mu_3\text{-}\sigma\text{:}\eta^6\text{-}7,9\text{-}Me_2\text{-}7,9\text{-}C_2B_{10}H_8\text{-}12\text{-}OC)(CO)_5(PMe_3)_2(\eta^5\text{-}C_5H_5)]$	brown	60	2062 (s), 1991 (vs), 1931 (m), 1890 (s), 1777 (m br)	26.47 (26.22)	3.24 (3.34)

[a] Measured in CH_2Cl_2 unless otherwise stated. All complexes show a weak, very broad absorption at ca. 2550 cm^{-1} due to cage BH stretches. [b] Calculated values in parentheses. [c] 1.89 (1.96), N. [d] 1.53 (1.85), N. [e] Measured in *n*-hexane.

Table II. Hydrogen-1 and Carbon-13 NMR Data[a]

compd	$^1H/\delta$	$^{13}C/\delta$[b]
2a[c]	1.86 (s, 6 H, CMe), 7.47–7.66 (m, 60 H, Ph)	229.9 (CO), 133.9 [C^4(Ph)], 132.3 [vt, C^2(Ph), $\lvert J(PC) + J(P'C)\rvert = 11$], 129.6 [vt, C^3 (Ph), $\lvert J(PC) + J(P'C)\rvert = 13$], 127.4 [d, C^1(Ph), $J(PC) = 109$], 54.7 (br, *C*Me), 36.8 (C*Me*)
2b[c]	1.96 (s, 6 H, CMe), 7.45–7.68 (m, 60 H, Ph)	223.4 (CO), 133.9 [C^4(Ph)], 132.3 [vt, C^2(Ph), $\lvert J(PC) + J(P'C)\rvert = 11$], 129.6 [vt, C^3(Ph), $\lvert J(PC) + J(P'C)\rvert = 13$], 127.4 [d, C^1(Ph), $J(PC) = 109$], 54.8 (br, *C*Me), 37.1 (C*Me*)
7a	1.72 (s, 3 H, CMe), 2.24 (s, 3 H, CMe), 2.11–2.75 (br, 16 H, CH_2), 4.54 [m, 1 H, CH, $J(PtH) = 75$], 4.85 (br, 3 H, CH), 5.23 [m, 1 H, CH, $J(PtH) = 32$], 5.35 [m, 1 H, CH, $J(PtH) = 30$], 5.54 [m, 1 H, CH, $J(PtH) = 40$], 5.88 [m, 1 H, CH, $J(PtH) = 40$]	216.5 [CO, $J(PtC) = 36, 127$], 126.1 [CH, $J(PtC) = 43$], 120.0 [CH, $J(PtC) = 32$], 117.8 [CH, $J(PtC) = 23$], 114.2 [CH, $J(PtC) = 12$], 91.4 [CH, $J(PtC) = 151$], 88.4 [CH, $J(PtC) = 177$], 83.9 [CH, $J(PtC) = 210$], 78.8 [CH, $J(PtC) = 197$], 69.6 (br, *C*Me), 67.8 (br, *C*Me), 38.7 [CH_2, $J(PtC) = 34$], 34.3 [CH_2, $J(PtC) = 25$], 34.0 (C*Me*), 33.8 (C*Me*), 32.3 [CH_2, $J(PtC) = 27$], 30.8 [CH_2, $J(PtC) = 35$], 29.7 [CH_2, $J(PtC) = 31$], 28.9 [CH_2, $J(PtC) = 20$], 27.9 [CH_2 $J(PtC) = 16$], 27.3 [CH_2, $J(PtC) = 14$]
7b	1.92 (s, 3 H, CMe), 2.40 (s, 3 H, CMe), 2.10–2.85 (br, 16 H, CH_2), 4.44 [m, 1 H, CH, $J(PtH) = 72$], 4.79 [m, 1 H, CH, $J(PtH) = 75$], 4.83 (m, 1 H, CH), 4.89 [m, 1 H, CH, $J(PtH) = 88$], 5.16 (m, 1 H, CH), 5.30 (m, 1 H, CH), 5.49 [m, 1 H, CH, $J(PtH) = 44$], 5.83 [m, 1 H, CH, $J(PtH) = 44$]	209.4 [CO, $J(PtC) = 39, 98$], 125.8 [CH, $J(PtC) = 47$], 119.8 [CH, $J(PtC) = 35$], 117.3 [CH, $J(PtC) = 25$], 114.1 [CH, $J(PtC) = 14$], 90.4 [CH, $J(PtC) = 147$], 87.4 [CH, $J(PtC) = 176$], 83.9 [CH, $J(PtC) = 204$], 78.9 [CH, $J(PtC) = 190$], 62.9 (vbr, 2 × *C*Me), 39.6 [CH_2, $J(PtC) = 36$], 34.3 [CH_2, $J(PtC) = 22$], 34.1 (C*Me*), 34.0 (C*Me*), 32.3 [CH_2, $J(PtC) = 26$], 30.8 [CH_2, $J(PtC) = 34$], 29.7 [CH_2, $J(PtC) = 29$], 28.7 [CH_2, $J(PtC) = 19$], 27.7 [CH_2, $J(PtC) = 16$], 27.0 [CH_2, $J(PtC) = 16$]
8a	−5.19 [br, 1 H, B–H→Pt, $J(PtH) = 666$], 1.65 (s, 3 H, CMe), 2.63 (s, 3 H, CMe), 7.20–7.79 (30 H, Ph)[d]	224.1 (vbr, MoCO), 217.0 (PtCO), 133.7–128.7 (Ph), 91.3 (br, *C*Me), 75.0 (br, *C*Me), 34.4 (C*Me*), 33.5 (C*Me*)[e]
8b	−5.00 [br, 1 H, B–H→Pt, $J(PtH) = 647$], 1.76 (s, 3 H, CMe), 2.82 (s, 3 H, CMe), 7.32–7.49 (30 H, Ph)[f]	206.4 (PtCO), 133.8–128.6 (Ph), 82.9 (br, *C*Me), 69.5 (br, *C*Me), 35.0 (C*Me*), 33.7 (C*Me*)[e,g]
9	1.69 (s, 3 H, CMe), 2.33 (s, 3 H, Me-4), 2.35 (s, 3 H, Me-4), 2.51 (s, 3 H, CMe), 5.38 (s, 5 H, C_5H_5), 5.73 (s, 5 H, C_5H_5), 6.85, 6.97 {$[AB]_2$, 4 H, C_6H_4, $J(AB) = 8$}, 7.17, 7.38 {$[AB]_2$, 4 H, C_6H_4, $J(AB) = 8$}	313.9 (μ-C), 313.1 (μ-C), 264.6 (μ-COB), 223.7 (CO), 221.6 (CO), 221.0 (CO), 220.1 (CO), 219.7 (CO), 216.3 (CO), 180.9 (PtCO), 152.7, 151.0 [$C^1(C_6H_4)$], 140.0, 138.6 [$C^4(C_6H_4)$], 129.8–125.5 [$C^{2,3}(C_6H_4)$], 96.8 (br, *C*Me), 96.1 (C_5H_5), 92.2 (C_5H_5), 73.2 (br, *C*Me), 35.3 (C*Me*), 26.4 (C*Me*), 21.8 (Me-4), 21.1 (Me-4)
	1.60 (s, 3 H, CMe), 2.28, 2.41, 2.48 (s × 3, 9 H, CMe and Me-4), 5.55 (s, 5 H, C_5H_5), 5.64 (s, 5 H, C_5H_5), 6.90, 7.06 {$[AB]_2$, 4 H, C_6H_4, $J(AB) = 8$}, 7.12, 7.21 {$[AB]_2$, 4 H, C_6H_4, $J(AB) = 8$}[h]	317.2 (μ-C), 311.6 (μ-C), 270.4 (μ-COB), 224.8 (CO), 223.6 (CO), 223.5 (CO), 220.9 (CO), 220.3 (CO), 218.9 (CO), 179.6 (PtCO), 153.3, 151.2 [$C^1(C_6H_4)$], 139.5, 138.8 [$C^4(C_6H_4)$], 129.8–125.5 [$C^{2,3}(C_6H_4)$], 96.6 (C_5H_5), 92.4 (C_5H_5), 91.6 (br, *C*Me), 67.8 (br, *C*Me), 35.1 (C*Me*), 26.3 (C*Me*), 21.7 (Me-4), 21.2 (Me-4)[h]
10	1.45 [d, 9 H, PMe_3, $J(PH) = 9$, $J(PtH) = 30$], 1.56 [d, 9 H, PMe_3, $J(PH) = 9$, $J(PtH) = 25$], 1.66 (s, 3 H, CMe), 2.32, 2.33 (s × 2, 6 H, CMe and Me-4), 5.24 (s, 5 H, C_5H_5), 6.97, 7.04 {$[AB]_2$, 4 H, C_6H_4, $J(AB) = 8$}	307.7 (μ-C), 257.2 (μ-COB), 221.8 (CO), 221.3 (2 × CO), 220.5 (CO), 185.6 (PtCO), 157.1 [$C^1(C_6H_4)$], 135.6 [$C^4(C_6H_4)$], 128.7, 127.0 [$C^{2,3}(C_6H_4)$], 96.8 (C_5H_5), 95.7 (br, *C*Me), 70.1 (br, *C*Me), 35.6 (C*Me*), 26.5 (C*Me*), 21.0 (Me-4), 18.8 [d, PMe_3, $J(PC) = 31$, $J(PtC) = 38$], 17.3 [d, PMe_3, $J(PC) = 31$, $J(PtC) = 35$]

[a] Measurements in CD_2Cl_2 at ambient temperatures unless otherwise stated. [b] Hydrogen-1 decoupled, chemical shifts are positive to high frequency of $SiMe_4$. [c] Data obtained from ambient temperature spectra, as low-temperature-limiting spectra could not be obtained. [d] Measured at 220 K. [e] Measured at 190 K. [f] Measured at 230 K. [g] Tungsten carbonyls not observed presumably due to dynamic behavior. [h] Signals due to minor isomer; see text.

evident from the ^{11}B NMR data (Table III). Thus two relatively deshielded signals, both of which are strongly coupled to ^{195}Pt, are observed in the spectrum of each species [**7a**, δ 45.7 and 36.7 ppm with $J(PtB) = 610$ and 598 Hz, respectively; **7b**, δ 42.6 and 34.7 ppm with $J(PtB) = 610$ and 598 Hz, respectively]. Furthermore, these signals remain singlets in proton-coupled spectra. In the $^{13}C\{^1H\}$ NMR spectra (Table II) of the two compounds, the signals arising from the olefin carbon atoms of the cod ligands occur in the range δ ca. 126–78 ppm and all show ^{195}Pt satellite peaks, as expected. Only one signal due to the three carbonyl ligands is seen in the $^{13}C\{^1H\}$ NMR spectrum throughout the temperature range 295–200 K, indicating rapid carbonyl site exchange. However, the time-averaged signal shows coupling to two ^{195}Pt nuclei [for **7a**, time-averaged $J(PtC) = 36$ and 127 Hz], implying that in the ground state structure one of the CO groups bridges a Pt–M (Mo or W) vector. In agreement with this, a band is observed at 1762 cm^{-1} in the IR spectra of both **7a** and **7b**.

Table III. Boron-11 and Phosphorus-31 NMR Data[a]

compd	$^{11}B/\delta$	$^{31}P/\delta$
2a	–0.2 (3 B), –7.4 (1 B), –10.0 (3 B), –11.4 (2 B), –17.3 (1 B)	
2b	–1.0 (3 B), –6.7 (1 B), –10.9 (5 B), –19.1 (1 B)	
7a	45.7 [1 B, B–Pt, *J*(PtB) = 610], 36.7 [1 B, B–Pt, *J*(PtB) = 598], 6.7 (1 B), –1.4 (1 B), –3.4 (1 B), –5.9 (1 B), –10.4 (2 B), –12.7 (1 B), –15.8 (1 B)	
7b	42.6 [1 B, B–Pt, *J*(PtB) = 610], 34.7 [1 B, B–Pt, *J*(PtB) = 598], 3.7 (1 B), –3.4 (2 B), –6.3 (1 B), –10.8 (2 B), –12.3 (1 B), –16.6 (1 B)	
8a	24.3 [1 B, B–H→Pt, *J*(HB) = 61], +1.5 to –18.2 (9 B)	60.4 [d, *J*(PP) = 8, *J*(PtP) = 479, 5650], 38.6 [br, *J*(PtP) = 439, 4384]
8b	20.3 [1 B, B–H→Pt, *J*(HB) = 60, *J*(PtB) = 79], +2.5 to –19.5 (9 B)	68.8 [d, *J*(PP) = 10, *J*(PtP) = 503, 5489], 32.3 [br, *J*(PtP) = 488, 4426]
9[b]	62.5 (br, 1 B, B–Pt), 17.1 (br, 1 B, B–O), –4.6, –8.2, –21.2 (8 B)	
10	56.4 [1 B, B–Pt, *J*(PtB) = 512], 15.4 (br, 1 B, B–O), –4.4 (4 B), –6.3 (1 B), –7.6 (1 B), –11.1 (1 B), –20.5 (1 B)	–13.0 [d, *J*(PP) = 17, *J*(PtP) = 3330], –20.1 [d, *J*(PP) = 17, *J*(PtP) = 3267]

[a] Measurements at ambient temperatures in CD_2Cl_2. Hydrogen-1 decoupled. Chemical shifts (ppm) are positive to high frequency of $BF_3\cdot Et_2O$ (external) and 85% H_3PO_4 (external), respectively. [b] Two isomers present; see text.

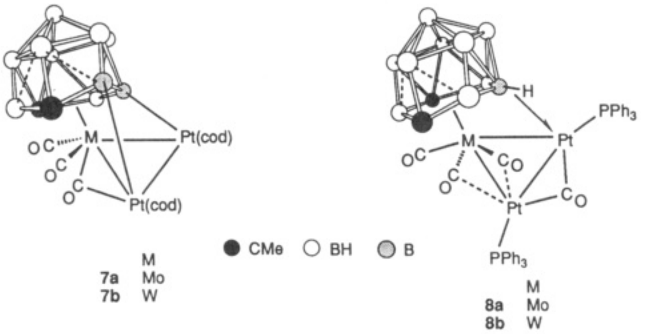

	M
7a	Mo
7b	W

	M
8a	Mo
8b	W

When similar methodology was employed, the trimetal compounds $[MPt_2(\mu\text{-}CO)(CO)_3(PPh_3)_2(\eta^6\text{-}7,9\text{-}Me_2\text{-}7,9\text{-}C_2B_{10}H_{10})]$ (**8a**, M = Mo; **8b**, M = W) were obtained from the salts **2**, *cis*-$[PtCl_2(CO)(PPh_3)]$, and $TlPF_6$. The molecular structure of these species has been confirmed by a single-crystal X-ray structure determination of **8a**. The molecule is shown in Figure 1, and selected bond distances and bond angles are given in Table IV. The core of the molecule consists of an almost isosceles triangle of metal atoms [Mo–Pt(1) 2.707(1) Å, Mo–Pt(2) 2.950(1) Å, Pt(1)–Pt(2) 2.747(1) Å; Pt(1)–Mo–Pt(2) 57.9(1)°, Mo–Pt(2)–Pt(1) 56.6(1)°, Mo–Pt(1)–Pt(2) 65.5(1)°] in which the longer of the Mo–Pt vectors is spanned by the carborane cage through a B–H→Pt "agostic" interaction. In addition to being ligated by the carborane cage the molybdenum is bound to three carbonyl groups, one of which is terminally bound [Mo–C(6)–O(6) 178.1(8)°] while the other two are both weakly interacting with Pt(1) [Pt(1)---C(5) 2.295(8) Å, Pt(1)---C(7) 2.329(8) Å, Mo–C(5)–O(5) 165.2(6)°, Mo–C(7)–O(7) 165.9(6)°]. Each platinum atom carries a triphenylphosphine ligand, and the Pt–Pt vector is essentially symmetrically bridged by a CO group [Pt(1)–C(8) 2.026(7) Å, Pt(2)–C(8) 1.996(8) Å, Pt(1)–C(8)–O(8) 132.2(6)°, Pt(2)–C(8)–O(8) 141.2(6)°]. Comparing the Mo–Pt distances in **8a** with that found [2.814(1) Å] in the dinuclear compound $[MoPt(CO)_4(PPh_3)(\eta^6\text{-}7,9\text{-}Me_2\text{-}7,9\text{-}C_2B_{10}H_{10})]$ (**4c**)[1] reveals that the distance in the latter is intermediate between the two distances found in **8a** but, somewhat surprisingly, is substantially shorter than the one [Mo–Pt(2)] spanned by the carborane cage (2.814 vs 2.950 Å).

The trimetal compounds **7** and **8** have a total of 46 and 44 cluster valence electrons, respectively, rather than 48, as is normally associated with a triangular geometry in which each metal center has a filled 18-electron shell. This is not unusual for cluster compounds in which one or more of the metal atoms is a platinum group metal since they have a preference for 16-electron complexes in their low oxidation states. Hence, planar triangular clusters containing platinum and having 42, 44, and 46 valence electrons are well documented.[4,5]

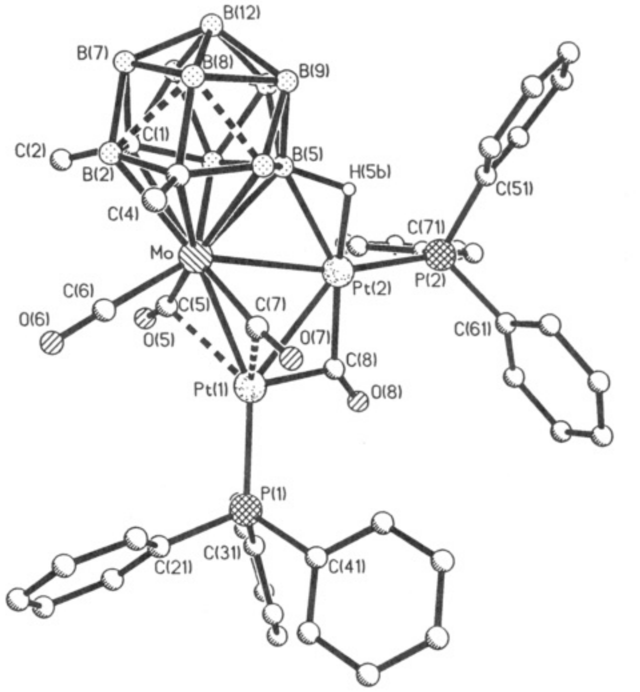

Figure 1. Structure of $[MoPt_2(\mu\text{-}CO)(CO)_3(PPh_3)_2(\eta^6\text{-}7,9\text{-}Me_2\text{-}7,9\text{-}C_2B_{10}H_{10})]$ (**8a**), showing the crystallographic labeling scheme.

The NMR spectral data for **8a** and **8b** are entirely consistent with the structure established in the solid state for **8a**. Thus the B–H→Pt agostic interaction gives rise to a broad signal in the proton spectra at ca. δ –5 ppm, with ^{195}Pt satellite peaks [*J*(PtH) ca. 650 Hz], and in the ^{11}B NMR spectra a relatively deshielded resonance at ca. δ 20 ppm. The phosphorus-31 NMR spectra of both compounds consist of a doublet signal and a broad signal. The broadness of the latter presumably results from unresolved coupling to boron, and therefore this signal is likely to be due to the PPh_3 ligand attached to the platinum atom of the B–H→Pt group. In the $^{13}C\{^1H\}$ NMR spectrum of **8a** a very broad resonance is observed for the three nonequivalent Mo–CO groups even at low temperatures, while the carbonyl group bridging the platinum atoms appears as a sharp singlet. Similarly, for **8b** a resonance

---

(4) *The Chemistry of Metal Cluster Complexes*; Shriver, D. F., Kaesz, H. D., Adams, R. D., Eds.; VCH Publishers: New York, 1990.

(5) Gilmour, D. I.; Mingos, D. M. P. *J. Organomet. Chem.* **1986**, *302*, 127.

Table IV. Selected Internuclear Distances (Å) and Angles (deg) for [MoPt$_2$(μ-CO)(CO)$_3$(PPh$_3$)$_2$(η^6-7,9-Me$_2$-7,9-C$_2$B$_{10}$H$_{10}$)] (8a), with Estimated Standard Deviations in Parentheses

Mo–Pt(1)	2.707(1)	Mo–Pt(2)	2.950(1)	Pt(1)–Pt(2)	2.747(1)	Pt(1)–P(1)	2.275(2)
Pt(2)–P(2)	2.268(2)	Mo–C(1)	2.506(7)	Mo–C(3)	2.270(7)	Mo–B(2)	2.452(8)
Mo–B(4)	2.431(9)	Mo–B(5)	2.325(9)	Mo–B(6)	2.368(8)	Mo–C(5)	2.056(8)
Pt(1)---C(5)	2.295(8)	C(5)–O(5)	1.141(10)	Mo–C(6)	2.022(8)	C(6)–O(6)	1.142(10)
Mo–C(7)	2.028(8)	C(7)–O(7)	1.150(11)	Pt(1)---C(7)	2.329(8)	Pt(1)–C(8)	2.026(7)
Pt(2)–C(8)	1.996(8)	C(8)–O(8)	1.150(9)	Pt(2)–B(5)	2.359(9)	Pt(2)–H(5b)	1.773
B(5)–H(5b)	1.281	C(1)–B(2)	1.697(11)	C(1)–B(6)	1.691(10)	C(1)–B(7)	1.700(11)
C(1)–B(11)	1.712(11)	B(2)–C(3)	1.570(13)	B(2)–B(7)	1.820(12)	B(2)---B(8)	2.050(13)
C(3)–B(4)	1.537(11)	C(3)–B(8)	1.763(12)	B(4)–B(5)	1.790(13)	B(4)---B(8)	1.942(12)
B(4)–B(9)	1.769(13)	B(5)–B(6)	1.763(14)	B(5)–B(9)	1.747(14)	B(5)–B(10)	1.727(14)
B(6)–B(10)	1.801(13)	B(6)–B(11)	1.805(12)	B(7)–B(8)	1.861(14)	B(7)–B(11)	1.720(12)
B(7)–B(12)	1.689(13)	B(8)–B(9)	1.874(12)	B(8)–B(12)	1.793(14)	B(9)–B(10)	1.738(15)
B(9)–B(12)	1.770(15)	B(10)–B(11)	1.753(13)	B(10)–B(12)	1.807(13)	B(11)–B(12)	1.758(15)

Mo–Pt(1)–Pt(2)	65.5(1)	Mo–Pt(2)–Pt(1)	56.6(1)	Pt(1)–Mo–Pt(2)	57.9(1)
Mo–B(5)–Pt(2)	78.1(3)	Mo–C(5)–Pt(1)	76.7(3)	Mo–C(5)–O(5)	165.2(6)
Pt(1)–C(5)–O(5)	117.7(5)	Mo–C(6)–O(6)	178.1(8)	Mo–C(7)–O(7)	165.9(6)
Mo–C(7)–Pt(1)	76.5(3)	Pt(1)–C(7)–O(7)	117.6(5)	Pt(2)–C(8)–O(8)	141.2(6)
Pt(1)–C(8)–O(8)	132.2(6)	Pt(2)–C(8)–Pt(1)	86.2(3)	Mo–Pt(1)–P(1)	149.1(1)
Mo–Pt(2)–P(2)	166.7(1)	Pt(1)–Pt(2)–P(2)	136.4(1)	Pt(2)–Pt(1)–P(1)	143.8(1)

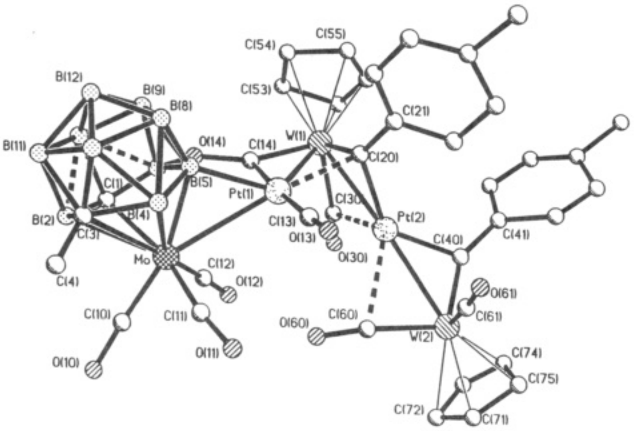

Figure 2. Structure of [MoW$_2$Pt$_2$(μ-CC$_6$H$_4$Me-4)(μ_3-CC$_6$H$_4$-Me-4)(μ_3-σ:η^6-7,9-Me$_2$-7,9-C$_2$B$_{10}$H$_8$-12-OC)(CO)$_7$(η^5-C$_5$H$_5$)$_2$] (**9**), showing the crystallographic labeling scheme.

at δ 206.4 ppm can be assigned to the Pt(μ-CO)Pt group but the signals due to the tungsten carbonyls are not observed. These observations are consistent with slow carbonyl site exchange at the molybdenum or tungsten metal centers. The cage CMe groups give rise to four signals, as expected.

Infrared measurements during the course of the reactions leading to the species **8** revealed that the anticipated dimetal compounds [MPt(CO)$_4$(PPh$_3$)(η^6-7,9-Me$_2$-7,9-C$_2$B$_{10}$H$_{10}$)] (**4c**, M = Mo; **4d**, M = W) are formed, but in very low yield (<10%). This together with the isolation of only the trinuclear metal species **7** from reactions between **2** and [PtCl$_2$(cod)] would seem to suggest that reactions between the salts **2** and the platinum complexes [PtCl$_2$(cod)] or [PtCl$_2$(CO)(PPh$_3$)], in the presence of TlPF$_6$, initially produce dinuclear metal species which are unstable toward attack by unreacted platinum complex, thereby affording the observed trimetal compounds. This in turn implies that the salts [PtH(PPh$_3$)$_3$][MPt(CO)$_4$(PPh$_3$)(μ-σ:η^6-7,9-Me$_2$-7,9-C$_2$B$_{10}$H$_9$)] (**6**), which were obtained from reactions of Na$_2$[M(CO)$_3$(η^6-7,9-Me$_2$-7,9-C$_2$B$_{10}$H$_{10}$)] with [PtCl$_2$(cod)] in the presence of triphenylphosphine,[1] are formed via the intermediacy of trimetal compounds, and that the hydride ligand present in the cation of these salts originates from a cage BH group.

The nature of the compounds **7** suggested that treatment with the alkylidyne complex [W(≡CC$_6$H$_4$Me-4)(CO)$_2$(η^5-C$_5$H$_5$)] might result in displacement of one or both of the cyclooctadiene ligands with formation of higher nuclearity metal species. This was borne out experimentally. Thus when [MoPt$_2$(μ-CO)(μ_3-σ,σ':η^6-7,9-Me$_2$-7,9-C$_2$B$_{10}$H$_8$)(CO)$_2$(cod)$_2$] (**7a**) is treated with ca. 2 mol equiv of [W(≡CC$_6$H$_4$-Me-4)(CO)$_2$(η^5-C$_5$H$_5$)] in CH$_2$Cl$_2$, it slowly reacts to give the pentanuclear compound [MoW$_2$Pt$_2$(μ-CC$_6$H$_4$Me-4)(μ_3-CC$_6$H$_4$Me-4)(μ_3-σ:η^6-7,9-Me$_2$-7,9-C$_2$B$_{10}$H$_8$-12-OC)(CO)$_7$(η^5-C$_5$H$_5$)$_2$] (**9**). Although it was apparent from the NMR data for this species (Tables II and III) that the cod ligands had not simply been replaced by the W≡CR groups, interpretation of the data was complicated by the presence of two isomers (ca. 3:1) and the molecular structure was not fully established until a single-crystal X-ray structural analysis had been carried out. Discussion of the NMR spectral data is therefore deferred until after the structure is described. The molecule is shown in Figure 2, and selected bond distances and bond angles are collected in Table V. The complex consists of an essentially planar chain of five metal atoms, Mo—Pt(1)—W(1)—Pt(2)—W(2) [maximum deviation from the MoPt$_2$W$_2$ plane Pt(1) 0.76 Å], with one edge-bridging and one triply-bridging tolylmethylidyne group. The Pt(1)—W(1) [2.733(3) Å] and Pt(2)—W(1) [2.739(3) Å] distances are identical,

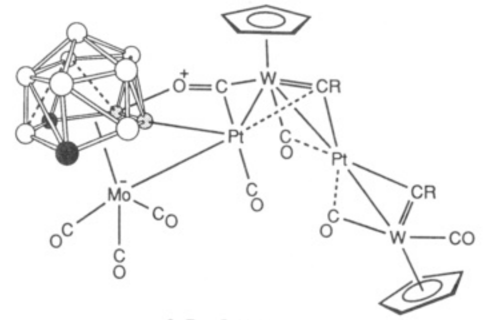

9 R = C$_6$H$_4$Me-4

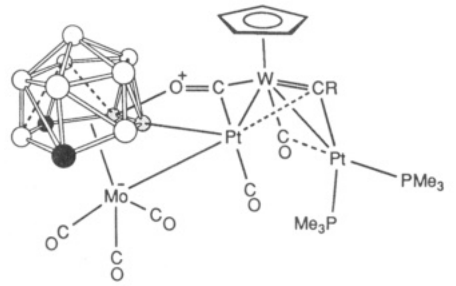

10 R = C$_6$H$_4$Me-4

Table V. Selected Internuclear Distances (Å) and Angles (deg) for $[MoW_2Pt_2(\mu\text{-}CC_6H_4Me\text{-}4)(\mu_3\text{-}CC_6H_4Me\text{-}4)(\mu_3\text{-}\sigma{:}\eta^6\text{-}7,9\text{-}Me_2\text{-}7,9\text{-}C_2B_{10}H_8\text{-}12\text{-}OC)(CO)_7(\eta^5\text{-}C_5H_5)_2]$ (9), with Estimated Standard Deviations in Parentheses

Mo–Pt(1)	3.012(5)	Mo–C(1)	2.337(37)	Mo–B(2)	2.425(44)	Mo–C(3)	2.516(45)
Mo–B(4)	2.330(52)	Mo–B(5)	2.129(60)	Mo–B(6)	2.476(46)	Mo–C(10)	1.921(42)
Mo–C(11)	1.963(36)	Mo–C(12)	1.873(44)	Pt(1)---Pt(2)	3.019(3)	Pt(1)–W(1)	2.733(3)
Pt(1)–B(5)	2.112(60)	Pt(1)–C(13)	1.940(39)	Pt(1)–C(14)	1.960(32)	Pt(1)---C(20)	2.201(42)
Pt(2)–W(1)	2.739(3)	Pt(2)–W(2)	2.726(3)	Pt(2)–C(20)	2.049(41)	Pt(2)---C(30)	2.276(43)
Pt(2)–C(40)	1.931(38)	Pt(2)---C(60)	2.554(39)	W(1)–C(14)	1.938(34)	W(1)–C(20)	1.985(40)
W(1)–C(30)	2.004(43)	W(2)–C(40)	1.787(35)	W(2)–C(60)	1.991(46)	W(2)–C(61)	1.797(42)
C(1)–B(2)	1.494(64)	C(1)–B(6)	1.443(63)	C(1)–B(10)	1.822(75)	B(2)–C(3)	1.798(68)
B(2)---B(10)	1.926(80)	B(2)–B(11)	1.909(82)	C(3)–B(4)	1.709(74)	C(3)–B(7)	1.666(83)
C(3)–B(11)	1.709(73)	B(4)–B(5)	1.840(70)	B(4)–B(7)	1.785(84)	B(4)–B(8)	1.937(76)
B(5)–B(6)	1.966(70)	B(5)–B(8)	1.698(72)	B(5)–B(9)	1.893(82)	B(6)–B(9)	1.830(70)
B(6)---B(10)	2.068(79)	B(6)–O(14)	1.337(51)	B(7)–B(8)	1.769(79)	B(7)–B(11)	1.807(87)
B(7)–B(12)	1.832(92)	B(8)–B(9)	1.760(67)	B(8)–B(12)	1.756(91)	B(9)–B(10)	1.675(81)
B(9)–B(12)	1.698(76)	B(10)–B(11)	1.755(96)	B(10)–B(12)	1.673(94)	B(11)–B(12)	1.691(100)
C(10)–O(10)	1.206(59)	C(11)–O(11)	1.210(47)	C(12)–O(12)	1.189(60)	C(13)–O(13)	1.180(54)
C(14)–O(14)	1.241(41)	C(20)–C(21)	1.502(56)	C(30)–O(30)	1.207(51)	C(40)–C(41)	1.536(54)
C(60)–O(60)	1.207(55)	C(61)–O(61)	1.247(63)				

Mo–C(10)–O(10)	177.6(31)	Mo–C(11)–O(11)	170.5(30)	Mo–C(12)–O(12)	170.1(41)
Mo–Pt(1)–W(1)	129.6(1)	Mo–B(5)–Pt(1)	90.5(23)	Mo–Pt(1)–B(5)	45.0(16)
Mo–Pt(1)–C(14)	87.5(11)	Mo–Pt(1)–Pt(2)	128.4(1)	Pt(2)–Pt(1)–C(14)	93.8(9)
Pt(1)–C(14)–W(1)	89.0(13)	Pt(1)–C(14)–O(14)	126.3(26)	W(1)–C(14)–O(14)	144.3(27)
B(6)–O(14)–C(14)	118.7(31)	Pt(2)–Pt(1)–B(5)	172.2(15)	W(1)–Pt(1)–B(5)	122.6(15)
Pt(1)–C(20)–W(1)	81.4(14)	Pt(1)–C(20)–Pt(2)	90.5(16)	Pt(2)–C(20)–W(1)	85.5(17)
Pt(1)–C(20)–C(21)	118.1(27)	W(1)–C(20)–C(21)	141.7(31)	Pt(2)–C(20)–C(21)	124.0(26)
Pt(1)–C(13)–O(13)	177.1(28)	Pt(2)–C(30)–W(1)	79.3(14)	W(1)–C(30)–O(30)	159.6(36)
Pt(2)–C(30)–O(30)	119.7(33)	Pt(1)–Pt(2)–W(1)	56.4(1)	Pt(1)–Pt(2)–W(2)	127.7(1)
Pt(1)–W(1)–Pt(2)	67.0(1)	W(1)–Pt(2)–W(2)	168.9(1)	Pt(1)–Pt(2)–C(40)	157.6(11)
W(2)–C(40)–C(41)	147.0(29)	Pt(2)–C(60)–W(2)	72.5(12)	Pt(2)–C(60)–O(60)	110.4(31)
W(2)–C(60)–O(60)	164.5(35)	W(2)–C(61)–O(61)	173.9(47)		

within experimental error, and longer than Pt(2)—W(2) [2.726(3) Å]. These distances should be compared with those in the compound $[W_3Pt_2(\mu\text{-}CC_6H_4Me\text{-}4)_2(\mu_3\text{-}CC_6H_4\text{-}Me\text{-}4)(CO)_6(\eta^5\text{-}C_5H_5)_3]$ for which the Pt—W distances involving the edge-bridging alkylidyne groups [Pt—W(av) 2.716 Å] are also shorter than those involving the triply-bridging alkylidyne group [Pt—W(av) 2.748 Å].[6] The Pt---Pt distance of 3.019(3) Å in **9** is similar to those observed in the compounds $[W_3Pt_2(\mu\text{-}CC_6H_4Me\text{-}4)_2(\mu_3\text{-}CC_6H_4Me\text{-}4)(CO)_6(\eta^5\text{-}C_5H_5)_3]$ [2.949(2) Å] and $[W_2Pt_3(\mu_3\text{-}CC_6H_4Me\text{-}4)_2(CO)_4(cod)_2(\eta^5\text{-}C_5H_5)_2]$ [3.089(1) Å].[6] The Mo—Pt distance of 3.012(5) Å is long but comparable with the Mo—Pt(2) distance in **8a**. Indeed, these distances appear to be among the longest Mo—Pt lengths so far observed.[1,7] For comparison, in the linear trimetallic carbene complex $[Mo_2Pt\{C(OEt)N(H)C_6H_{11}\}(CNC_6H_{11})(CO)_6(\eta^5\text{-}C_5H_5)_2]$ both Mo—Pt distances are 2.889(2) Å,[8] while in the triangulated species $[MoPt_2(\mu_3\text{-}As)(CO)_4(PPh_3)_2(\eta^5\text{-}C_5H_5)]$ the Mo–Pt distances are 2.777(3) and 2.799(3) Å.[9]

The contact carbon atom of the triply-bridging tolylmethylidyne group C(20) is essentially equidistant from the two metal atoms W(1) and Pt(2) [C(20)–W(1) 1.99(4) Å, C(20)–Pt(2) 2.05(4) Å] but is situated appreciably further away from Pt(1) [C(20)–Pt(1) 2.20(4) Å]. The terminal Pt(2)–W(2) vector is asymmetrically bridged by the atom C(40) at distances [C(40)–Pt(2) 1.93(4) Å, C(40)–W(2) 1.79(4) Å] similar to those observed in related compounds containing an edge-bridging tolylmethylidyne group.[6,10] Whereas the molybdenum atom carries three terminal carbonyl groups [average Mo–C–O 173°] and Pt(1) carries one such group [Pt(1)–C(13)–O(13) 177(3)°], both of the Pt(2)–W vectors are semibridged by CO groups [W(1)–C(30)–O(30) 160(4)°, W(2)–C(60)–O(60) 165(4)°]. In addition, the tungsten atom at the end of the chain is bound to a terminal CO ligand [W(2)–C(61)–O(61) 174(5)°].

As expected, the C_2B_{10} carborane cage is bound to Mo in the usual hexahapto manner in which the distances between molybdenum and the atoms forming the open $\overline{\text{CBCBBB}}$ ring of the cage vary substantially. Thus, the atom C(1) which is in the site of lowest connectivity of all the cage atoms is situated ca. 0.2 Å closer to the metal than C(3). The distances between the lower and upper belts of the cage involving the high-coordinate atom B(10) are relatively long [B(2)---B(10) 1.93(8) Å, B(6)---B(10) 2.07(8) Å], and this leads to two approximately square faces defined by the atoms C(1)B(6)B(9)B(10) and C(1)B(2)B(11)B(10). This is a feature common to most compounds containing this cage system and does not warrant further comment.[11] However, in the structure of **9** the adjacent atoms B(5) and B(6) are both involved in exopolyhedral bonding, and this appears to place extra geometrical constraints upon the cage, resulting in further distortions. Thus the distances B(2)–B(11) [1.91(8) Å] and B(4)–B(8) [1.94(8) Å], between atoms in the lower and upper belts of the cage are also longer than is normally observed, as is the B(5)–B(6) distance of 1.97(7) Å.

The atom B(5) forms an exopolyhedral B–Pt σ-bond, as expected, since there are two such interactions in the parent compound **7a**. The B(5)–Pt(1) distance of 2.11(6) Å is similar to that [2.15(1) Å] found in the complex $[WPt(\mu\text{-}CC_6H_4Me\text{-}4)(\mu\text{-}\sigma{:}\eta^6\text{-}7,9\text{-}Me_2\text{-}7,9\text{-}C_2B_{10}H_9)(CO)_2(PMe_2\text{-}$

---

(6) Elliott, G. P.; Howard, J. A. K.; Mise, T.; Moore, I.; Nunn, C. M.; Stone, F. G. A. *J. Chem. Soc., Dalton Trans.* **1986**, 2091.

(7) (a) Braunstein, P.; Dusausoy, Y.; Fischer, J.; Jud, J-M.; *Organometallics* **1983**, *2*, 180. (b) Bars, O.; Braunstein, P.; *Angew. Chem., Int. Ed. Engl.* **1982**, *21*, 308. (c) Bender, R.; Braunstein, P.; Dusausoy, Y.; Protas, J. *J. Organomet. Chem.* **1979**, *172*, C51.

(8) Braunstein, P.; Keller, K.; Vahrenkamp, H. *J. Organomet. Chem.* **1979**, *165*, 233.

(9) Bohn, T.; Gorzellik, M.; Nuber, B.; Ziegler, M. L. *J. Organomet. Chem.* **1992**, *429*, 173.

(10) Ashworth, T. V.; Chetcuti, M. J.; Howard, J. A. K.; Stone, F. G. A.; Wisbey, S. J.; Woodward, P. *J. Chem. Soc., Dalton Trans.* **1981**, 763.

(11) Carr, N.; Fernandez, J. R.; Stone, F. G. A. *Organometallics* **1991**, *10*, 2718 and references therein.

Ph)$_2$],[12] and in both compounds it is the boron vertex β to the carbon vertices of the CBCB*B*B belt that is involved in this interaction. However, the second B–Pt bond present in **7a** has cleaved to allow Pt(2) and its associated ligand set to rotate away from the metallacarborane moiety, presumably to relieve steric interactions between the carborane cage, the cyclopentadienyl ligands, and the tolylmethylidyne groups. As a consequence of the cleavage of this bond, the boron atom involved has become attached to the oxygen atom of what was a tungsten carbonyl [B(6)–O(14) 1.34(5) Å, O(14)–C(14) 1.24(4) Å]. The carbon atom of this group, C(14), is roughly equidistant from W(1) and Pt(1) [C(14)–W(1) 1.94(3) Å, C(14)–Pt(1) 1.96(3) Å]. The structural parameters for this moiety suggest that the C(14)–O(14) bond has retained some multiple bond character.[13] For simplicity we have therefore chosen to depict the compound as zwitterionic, with a formal positive charge on the oxygen atom and a negative charge on the molybdenum atom. As far as we are aware this type of interaction has not previously been observed in metallacarborane chemistry.

We mentioned earlier that compound **9** is formed as a mixture of two isomers, in a ca. 3:1 ratio, as deduced from the NMR spectral data. The isomerization surely arises from the direction of addition of the W≡CR fragments to the platinum atoms, a feature common to this area of chemistry in which compounds containing chains of metal atoms are built up by the addition of alkylidyne complexes to platinum atoms. We have discussed this aspect in detail previously.[6] In the formation of **9** the orientation of the W(1)–C(20) vector is probably determined by the formation of the B(6)O(14)C(14)W(1) linkage, and so the isomerization most likely arises from the two possible ways in which the other W≡CR fragment attaches to Pt(2), depicted as **A** and **B**. The structure of **9** as determined by the X-ray study would then correspond to isomer **A**, which is therefore assumed to be the dominant isomer.

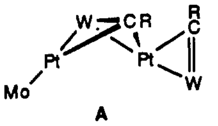

A

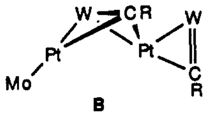

B

In the $^{13}C\{^1H\}$ NMR spectrum of **9** (Table II) the alkylidyne carbon atoms give rise to signals at δ 313.9 and 313.1 ppm (δ 317.2 and 311.6 ppm for the minor isomer **B**). That the signal due to the triply-bridging carbon atom occurs at such low field is indicative of only a weak interaction with one of the platinum atoms, as observed in the crystal structure. For comparison, the signals due to the triply-bridging alkylidyne carbon atoms in the complex [$W_3Pt_2(\mu$-CC_6H_4Me-4)$_2$(μ_3-CC_6H_4Me-4)(CO)$_6$(η^5-C_5H_5)$_3$] (two isomers) occur at δ ca. 260 ppm.[6] The resonance due to the carbon nucleus of the bridging COB group in **9** occurs at δ 264.6 ppm (δ 270.4 ppm for isomer **B**), that of the Pt–CO group occurs at δ 180.9 (δ 179.6 ppm for **B**) ppm, and those for the six other CO ligands occur between δ 223.7 and 216.3 ppm (δ 224.8 and 218.9 ppm for **B**). The remainder of the spectrum is as expected with four signals for the cage CMe nuclei of **A** at δ 96.8, 73.2 (CMe) and 35.3, 26.4 ppm (C*Me*) [δ 91.6, 67.8 (CMe) and 35.1, 26.3 ppm (C*Me*) for **B**]. The boron atoms of the B–OC linkages of the two isomers are evidenced by a broad signal at δ 17.1 ppm in the $^{11}B\{^1H\}$ spectrum, while those of the B–Pt σ-bonds give rise to a deshielded signal at δ 62.5 ppm.

In thf, complex **9** reacts instantaneously with PMe_3 to give [$MoWPt_2(\mu_3$-CC_6H_4Me-4)(μ_3-σ:η^6-7,9-Me_2-7,9-$C_2B_{10}H_8$-12-OC)(CO)$_5$(PMe_3)$_2$(η^5-C_5H_5)] (**10**), formed as a single isomer and characterized by NMR spectroscopy. Thus the $^{31}P\{^1H\}$ NMR spectrum (Table III) consists of two doublet signals at δ −13.0 and −20.1 ppm [J(PP) = 17 Hz] with ^{195}Pt satellite peaks, while the $^{11}B\{^1H\}$ spectrum has resonances at δ 56.4 [J(PtB) = 512 Hz] and 15.4 ppm due to the B–Pt and the B–OC linkages, respectively. Accordingly, the latter group gives rise to a signal at δ 257.2 ppm in the $^{13}C\{^1H\}$ NMR spectrum, and the edge-bridging tolylmethylidyne group is evidenced by a resonance at δ 307.7 ppm. Signals at δ 95.7, 70.1 and 35.6, 26.5 ppm are due to the cage CMe and C*Me* nuclei, respectively. That a single isomer is obtained from this reaction in which the edge-bridging tolylmethylidyne group of **9** has been displaced as [W(≡CC_6H_4Me-4)(CO)$_2$(η^5-C_5H_5)] would seem to confirm that the isomerization observed for **9** does indeed stem from the direction of attachment of the terminal W≡CC_6H_4Me-4 group, as proposed above.

The new cluster compounds described herein, and derived from the salts **2**, further demonstrate the synthetic potential of these and the related species **1** as reagents for preparing polynuclear metal–metal bonded complexes. The presence of the reactive carborane cage ligand in close proximity to the newly formed metal–metal interactions can lead to interesting reactions, affording species with novel structural types, as exemplified by the pentanuclear cluster **9**. Further studies in this area are currently underway.

Experimental Section

General Considerations. Solvents were distilled from appropriate drying agents under nitrogen prior to use. Petroleum ether refers to that fraction of boiling point 40–60 °C. All reactions were carried out under an atmosphere of dry nitrogen using Schlenk-line techniques. Chromatography columns (ca. 15 cm in length and ca. 2 cm in diameter) were packed with alumina (Brockmann activity II). The compounds [M(CO)$_3$(NCEt)$_3$] (M = Mo or W),[14] [$PtCl_2$(cod)],[15] *cis*-[$PtCl_2$(CO)(PPh_3)],[16] and [W(≡CC_6H_4Me-4)(CO)$_2$(η^5-C_5H_5)][17] were prepared as previously described. The NMR spectra were recorded in CD_2Cl_2 solvent at the following frequencies: ^1H at 360.13 MHz, ^{13}C at 90.56 MHz, ^{31}P at 145.78 MHz, and ^{11}B at 115.55 MHz.

Synthesis of the Salts [N(PPh_3)$_2$]$_2$[M(CO)$_3$(η^6-7,9-Me_2-7,9-$C_2B_{10}H_{10}$)] (2). In a typical experiment, a thf (30 mL) solution of Na_2[*nido*-7,9-Me_2-7,9-$C_2B_{10}H_{10}$] (5.98 mmol) [generated in situ from 1,2-Me_2-1,2-$C_2B_{10}H_{10}$ (1.03 g, 5.98 mmol), Na (ca. 0.40 g), and naphthalene (0.05 g)] was added to solid [Mo(CO)$_3$(NCEt)$_3$] (2.06 g, 5.97 mmol) and the resulting mixture was rapidly stirred for ca. 10 min. Solid [N(PPh_3)$_2$]Cl (6.85 g, 11.93 mmol) was then added and stirring was continued for a further 20 min, after which the solvent was removed in vacuo and the residue extracted with CH_2Cl_2 (50 mL). The extract was filtered through a Celite pad (ca. 5 cm), solvent volume was reduced in vacuo to ca. 10 mL, and Et_2O (20 mL) was added to give an oily precipitate which was washed with Et_2O (2 × 20 mL) and dried in vacuo for 16 h to give [N(PPh_3)$_2$]$_2$[Mo(CO)$_3$(η^6-7,9-Me_2-7,9-$C_2B_{10}H_{10}$)] (**2a**) (7.08 g) as a yellow powder. The salt obtained in this manner

---

[12] Carr, N.; Gimeno, M. C.; Stone, F. G. A. *J. Chem. Soc., Dalton Trans.* **1990**, 2617.

[13] Orpen, A. G.; Brammer, L.; Allen, F. H.; Kennard, O.; Watson, D. G.; Taylor, R. *J. Chem. Soc., Dalton Trans.* **1989**, S1.

[14] Kubas, G. J.; Van Der Sluys, L. S. *Inorg. Synth.* **1990**, *28*, 29.

[15] McDermott, J. X.; White, J. F.; Whitesides, G. M. *J. Am. Chem. Soc.* **1976**, *98*, 6521.

[16] Orchin, M.; Rycheck, M.; Smithies, A. C. *J. Organomet. Chem.* **1968**, *12*, 199.

[17] Fischer, E. O.; Lindner, T. L.; Huttner, G.; Friedrich, P.; Kreissl, F. R.; Besenhard, J. O. *Chem. Ber.* **1977**, *110*, 3397. Uedelhoven, W.; Eberl, K.; Kreissl, F. R. *Chem. Ber.* **1979**, *112*, 3376.

was sufficiently pure for use in most cases. Analytically pure samples can be obtained, but with considerable loss of product, by washing with thf and repeated recrystallization from CH_2Cl_2/Et_2O.

Similarly, $Na_2[\textit{nido}\text{-}7,9\text{-}Me_2\text{-}7,9\text{-}C_2B_{10}H_{10}]$ (5.75 mmol), $[W(CO)_3(NCEt)_3]$ (2.49 g, 5.75 mmol), and $[N(PPh_3)_2]Cl$ (6.60 g, 11.50 mmol) in thf (30 mL) gave $[N(PPh_3)_2]_2[W(CO)_3(\eta^6\text{-}7,9\text{-}Me_2\text{-}7,9\text{-}C_2B_{10}H_{10})]$ (**2b**) (7.07 g) as an orange powder.

Synthesis of the Complexes $[MPt_2(\mu\text{-}CO)(\mu_3\text{-}\sigma,\sigma'\text{:}\eta^6\text{-}7,9\text{-}Me_2\text{-}7,9\text{-}C_2B_{10}H_8)(CO)_2(cod)_2]$ (7). The compounds **2a** (0.50 g, 0.35 mmol), $[PtCl_2(cod)]$ (0.13 g, 0.35 mmol), and $TlPF_6$ (0.30 g, 0.86 mmol) were dissolved/suspended in thf (20 mL), and the resulting mixture was stirred for 16 h. Volatile materials were removed in vacuo, the residue was extracted with CH_2Cl_2–petroleum ether (1:1, 10 mL), and the extract was transferred to the top of a chromatography column packed with alumina. Eluting the column with the same solvent mixture removed an orange solution, from which $[MoPt_2(\mu\text{-}CO)(\mu_3\text{-}\sigma,\sigma'\text{:}\eta^6\text{-}7,9\text{-}Me_2\text{-}7,9\text{-}C_2B_{10}H_8)(CO)_2(cod)_2]$ (**7a**) was precipitated as an orange powder (0.08 g) by reducing the volume of solvent to ca. 5 mL.

The compound $[WPt_2(\mu\text{-}CO)(\mu_3\text{-}\sigma,\sigma'\text{:}\eta^6\text{-}7,9\text{-}Me_2\text{-}7,9\text{-}C_2B_{10}H_8)(CO)_2(cod)_2]$ (**7b**) (0.05 g) was similarly obtained from $[N(PPh_3)_2]_2[W(CO)_3(\eta^6\text{-}7,9\text{-}Me_2\text{-}7,9\text{-}C_2B_{10}H_{10})]$ (**2b**) (0.36 g, 0.24 mmol), $[PtCl_2(cod)]$ (0.09 g, 0.24 mmol), and $TlPF_6$ (0.20 g, 0.57 mmol).

Synthesis of the Complexes $[MPt_2(\mu\text{-}CO)(CO)_3(PPh_3)_2(\eta^6\text{-}7,9\text{-}Me_2\text{-}7,9\text{-}C_2B_{10}H_{10})]$ (8). To a mixture of **2a** (0.55 g, 0.39 mmol), *cis*-$[PtCl_2(CO)(PPh_3)]$ (0.22 g, 0.40 mmol), and $TlPF_6$ (0.30 g, 0.86 mmol) was added thf (25 mL), and the resulting solution/suspension was vigorously stirred for 20 h. Solvent was then removed in vacuo, the residue was extracted with CH_2Cl_2–petroleum ether (1:3, 8 mL), and the extract was chromatographed on alumina. Elution of the column with the same solvent mixture removed an orange fraction which was reduced in volume in vacuo to ca. 4 mL, and *n*-hexane (25 mL) was added. Reducing the volume of solvent again gave $[MoPt_2(\mu\text{-}CO)(CO)_3(PPh_3)_2(\eta^6\text{-}7,9\text{-}Me_2\text{-}7,9\text{-}C_2B_{10}H_{10})]$ (**8a**) as a red powder (0.12 g). Infrared measurements during the course of the reaction showed that the compound $[MoPt(CO)_4(PPh_3)(\eta^6\text{-}7,9\text{-}Me_2\text{-}7,9\text{-}C_2B_{10}H_{10})]$ (**4c**) was also formed in ca. 10% yield.

Employing $[N(PPh_3)_2]_2[W(CO)_3(\eta^6\text{-}7,9\text{-}Me_2\text{-}7,9\text{-}C_2B_{10}H_{10})]$ (**2b**) (0.52 g, 0.34 mmol), *cis*-$[PtCl_2(CO)(PPh_3)]$ (0.20 g, 0.36 mmol), and $TlPF_6$ (0.26 g, 0.74 mmol) in thf (25 mL) gave $[WPt_2(\mu\text{-}CO)(CO)_3(PPh_3)_2(\eta^6\text{-}7,9\text{-}Me_2\text{-}7,9\text{-}C_2B_{10}H_{10})]$ (**8b**) as a red powder (0.08 g), after column chromatography on alumina eluting with CH_2Cl_2–petroleum ether (1:1). Infrared measurements during the course of this reaction showed the presence of only a trace (<5%) of the compound $[WPt(CO)_4(PPh_3)(\eta^6\text{-}7,9\text{-}Me_2\text{-}7,9\text{-}C_2B_{10}H_{10})]$ (**4d**).

Reaction between $[MoPt_2(\mu\text{-}CO)(\mu_3\text{-}\sigma,\sigma'\text{:}\eta^6\text{-}7,9\text{-}Me_2\text{-}7,9\text{-}C_2B_{10}H_8)(CO)_2(cod)_2]$ (7a) and $[W(\equiv CC_6H_4Me\text{-}4)(CO)_2(\eta^5\text{-}C_5H_5)]$. A CH_2Cl_2 (15 mL) solution containing **7a** (0.23 g, 0.24 mmol) and $[W(\equiv CC_6H_4Me\text{-}4)(CO)_2(\eta^5\text{-}C_5H_5)]$ (0.20 g, 0.49 mmol) was stirred for 2 days at room temperature. Volatile materials were removed in vacuo, the residue was extracted with CH_2Cl_2–petroleum ether (1:2, 10 mL), and the extract was transferred to the top of an alumina chromatography column. Eluting the column with the same solvent mixture removed a purple solution which was reduced in volume in vacuo to ca. 5 mL to yield $[MoW_2Pt_2(\mu\text{-}CC_6H_4Me\text{-}4)(\mu_3\text{-}CC_6H_4Me\text{-}4)(\mu_3\text{-}\sigma\text{:}\eta^6\text{-}7,9\text{-}Me_2\text{-}7,9\text{-}C_2B_{10}H_8\text{-}12\text{-}OC)(CO)_7(\eta^5\text{-}C_5H_5)_2]$ (**9**) as a purple powder (0.10 g).

Reaction between $[MoW_2Pt_2(\mu\text{-}CC_6H_4Me\text{-}4)(\mu_3\text{-}CC_6H_4Me\text{-}4)(\mu_3\text{-}\sigma\text{:}\eta^6\text{-}7,9\text{-}Me_2\text{-}7,9\text{-}C_2B_{10}H_8\text{-}12\text{-}OC)(CO)_7(\eta^5\text{-}C_5H_5)_2]$ (9) and PMe_3. A thf (15 mL) solution of **9** (0.14 g, 0.09 mmol) was treated with PMe_3 (0.1 mL of a 0.5 M solution in thf) to give a brown solution which was evaporated to dryness in vacuo. The residue was extracted with CH_2Cl_2–petroleum ether (1:2, 5 mL), and the extract transferred to the top of an alumina chromatography column. Eluting the column with the same solvent mixture first removed $[W(\equiv CC_6H_4Me\text{-}4)(CO)_2(\eta^5\text{-}C_5H_5)]$ (identified by infrared spectroscopy) followed by a brown solution. Reducing the volume of solvent from the latter to ca. 5 mL in vacuo gave brown microcrystals of $[MoWPt_2(\mu_3\text{-}CC_6H_4Me\text{-}4)(\mu_3\text{-}\sigma\text{:}\eta^6\text{-}7,9\text{-}Me_2\text{-}7,9\text{-}C_2B_{10}H_8\text{-}12\text{-}OC)(CO)_5(PMe_3)_2(\eta^5\text{-}C_5H_5)]$ (**10**) (0.07 g).

Table VI. Data for X-ray Crystal Structure Analyses[a]

compd	**8a**	**9**
cryst dimens/mm	0.43 × 0.43 × 0.34	0.28 × 0.12 × 0.07[b] 0.39 × 0.16 × 0.10
formula	$C_{44}H_{46}B_{10}MoO_4P_2Pt_2$	$C_{38}H_{38}B_{10}MoO_8Pt_2W_2$
M_r	1295.03	1584.65
cryst color, shape	red prism	purple prism
cryst system	monoclinic	orthorhombic
space group (No.)	$P2_1/n$ (No. 14)	*Pbcn* (No. 60)
a/Å	13.047(2)	29.736(4)
b/Å	13.856(2)	18.077(1)
c/Å	27.103(6)	18.100(2)
β/deg	102.13(2)	
V/Å^3	4789.9(15)	9729.6(17)
Z	4	8
d_{calcd}/g cm^{-3}	1.796	2.163
μ(Mo Kα)/cm^{-1}	62.46	108.96
$F(000)$/e	2480	5808
2θ range/deg	3–40	3–40
T/K	292	292
no. of reflns meas	4977	5360
no. of unique reflns	4450	4544
no. of obsd reflns	3856	2665
criterion for observed n [$F_0 \geq n\sigma(F_0)$]	$n = 4$	$n = 4$
$R(R')$[c]	0.0235 (0.0277)	0.0755 (0.0800)
final electron density diff features (max/min)/e Å^{-3}	0.68/–0.39	2.20/–3.45
S (goodness-of-fit)	1.19	1.13

[a] Data collected on an Enraf-Nonius CAD4-F automated diffractometer operating in the ω–2θ scan mode (h 0–12, k 0–13, l –26 to +25 for **8a**; h 0–28, k 0–17, l 0–17 for **9**); graphite monochromated Mo Kα X-radiation, $\bar{\lambda} = 0.710\,73$ Å. Refinement was by block full matrix least squares on F with a weighting scheme of the form $w^{-1} = [\sigma^2(F_o) + g|F_o|^2]$ ($g = 0.0003$ for **8a**, 0.0079 for **9**) where $\sigma_c{}^2(F_o)$ is the variance in F_o due to counting statistics. [b] Two crystals used for data collection; see text. [c] $R = \sum||F_o| - |F_c||/\sum|F_o|$, $R' = \sum w^{1/2}||F_o| - |F_c||/\sum w^{1/2}|F_o|$.

Crystal Structure Determinations and Refinements. The crystal data and other experimental parameters for compounds **8a** and **9** are collected in Table VI. Crystals of compound **8a** were grown as red prisms by the slow diffusion of *n*-hexane into a concentrated CH_2Cl_2 solution of the complex at ca. –20 °C. Deep purple colored irregular prisms of compound **9** were obtained by prolonged cooling (ca. –20 °C) of a saturated solution of the complex in *n*-hexane. For each data set, final cell dimensions were determined from the setting angle values of 25 accurately centered reflections. Because of the small size of the crystals of **9** and slow decomposition in the X-ray beam, as well as the relatively large unit cell dimensions, reflections were collected from two independent crystals in order to obtain a sufficient number of data to give an accurate solution. Three standard reflections measured very 2 h showed no significant variation over the period of the data collection for compound **8a** (<0.8%). A gradual decrease in the intensity of the standard reflections for compound **9** (ca. 0.4% h^{-1} for crystal 1, ca. 0.1% h^{-1} for crystal 2) necessitated the application of a relevant decay correction. After deletion of these check intensity data as well as the systematic absences, averaging the duplicate and equivalent measurements was performed and the data were corrected for Lorentz, polarization, and X-ray absorption effects. The absorption corrections were based on empirical methods.

The structures were solved by conventional heavy-atom methods to determine the metal atom positions, and Fourier difference syntheses were used to locate all other non-hydrogen atoms, which were refined with anisotropic thermal parameters. For **8a**, the atom H(5b) was located in difference Fourier syntheses and allowed to ride on the atom B(5) with a fixed isotropic thermal parameter (U_{iso} 80 × 10^{-3} Å^2), all other hydrogen atoms were included at geometrically calculated positions (C–H 0.96 Å, B–H 1.10 Å) and allowed to ride on the parent carbon or boron atom with fixed isotropic thermal parameters (U_{iso} 80 × 10^{-3} Å^2). All hydrogen atoms for compound **9** were included at geometrically calculated positions (C–H 0.96 Å, B–H 1.10 Å) and allowed to ride on the parent carbon or boron atom with fixed isotropic thermal parameters (U_{iso} 80 and 60 × 10^{-3} Å^2, respectively). All

Table VII. Atomic Coordinates ($\times10^4$) and Equivalent Isotropic Displacement Parameters ($Å^2 \times 10^3$) for 8a

name	*x*	*y*	*z*	*U*(eq)[a]
Mo	2141(1)	3093(1)	9352(1)	30(1)
Pt(1)	1187(1)	1435(1)	8977(1)	35(1)
Pt(2)	483(1)	3056(1)	8425(1)	31(1)
P(1)	1168(1)	−207(2)	8961(1)	39(1)
P(2)	−784(2)	3405(1)	7738(1)	35(1)
C(1)	1922(5)	4516(5)	9890(3)	38(1)
B(2)	3203(6)	4304(7)	9890(3)	42(1)
C(3)	3570(5)	4048(5)	9390(3)	45(1)
B(4)	2896(7)	4270(6)	8865(3)	41(1)
B(5)	1509(7)	4361(7)	8811(3)	50(1)
B(6)	983(7)	4406(5)	9359(3)	37(1)
B(7)	2668(7)	5519(6)	9880(3)	44(1)
B(8)	3338(7)	5301(7)	9348(3)	53(1)
B(9)	2252(7)	5398(7)	8776(4)	59(1)
B(10)	1085(7)	5465(7)	8987(3)	53(1)
B(11)	1338(7)	5567(6)	9646(4)	51(1)
B(12)	2237(8)	6088(7)	9324(4)	62(1)
C(2)	1677(6)	4280(6)	10405(3)	65(1)
C(4)	4694(6)	3675(6)	9437(4)	72(1)
C(5)	986(6)	2413(5)	9633(3)	42(1)
O(5)	344(4)	2219(4)	9844(2)	64(1)
C(6)	3106(6)	2306(6)	9884(3)	54(1)
O(6)	3663(5)	1852(5)	10174(2)	78(1)
C(7)	2689(6)	2233(5)	8859(3)	44(1)
O(7)	3154(5)	1891(4)	8587(2)	73(1)
C(8)	−103(6)	1728(5)	8437(3)	46(1)
O(8)	−843(5)	1286(4)	8276(2)	79(1)
C(21)	2047(5)	−726(5)	9500(3)	45(1)
C(22)	1712(6)	−1269(5)	9850(3)	52(1)
C(23)	2384(6)	−1650(6)	10271(3)	71(1)
C(24)	3441(6)	−1443(6)	10335(4)	83(1)
C(25)	3814(8)	−896(8)	9988(4)	104(1)
C(26)	3108(5)	−538(7)	9572(4)	94(1)
C(31)	−73(5)	−803(5)	8959(3)	36(1)
C(32)	−266(6)	−1745(5)	8797(3)	50(1)
C(33)	−1207(6)	−2174(6)	8805(3)	54(1)
C(34)	−1976(7)	−1670(6)	8969(3)	68(1)
C(35)	−1795(6)	−752(7)	9148(3)	70(1)
C(36)	−847(6)	−296(6)	9138(3)	56(1)
C(41)	1597(5)	−691(5)	8414(3)	41(1)
C(42)	1456(6)	−163(6)	7976(3)	53(1)
C(43)	1715(6)	−547(5)	7554(3)	68(1)
C(44)	2114(6)	−1467(5)	7553(3)	60(1)
C(45)	2280(7)	−2010(6)	7988(3)	62(1)
C(46)	2021(6)	−1616(6)	8417(3)	60(1)
C(51)	−595(5)	4522(5)	7437(3)	44(1)
C(52)	391(7)	4825(6)	7409(3)	75(1)
C(53)	605(7)	5624(6)	7142(3)	86(1)
C(54)	−229(6)	6188(7)	6906(4)	87(1)
C(55)	−1236(7)	5933(8)	6935(4)	108(1)
C(56)	−1403(6)	5126(6)	7223(3)	84(1)
C(61)	−890(5)	2521(5)	7237(3)	44(1)
C(62)	−170(7)	2541(7)	6926(3)	82(1)
C(63)	−157(8)	1841(8)	6568(4)	97(1)
C(64)	−859(7)	1111(7)	6512(3)	78(1)
C(65)	−1631(7)	1086(6)	6791(3)	72(1)
C(66)	−1610(6)	1786(6)	7156(3)	56(1)
C(71)	−2059(5)	3479(5)	7895(3)	36(1)
C(72)	−2160(6)	3494(5)	8395(3)	49(1)
C(73)	−3106(5)	3551(6)	8532(3)	56(1)
C(74)	−4017(6)	3608(6)	8164(3)	61(1)
C(75)	−3942(7)	3588(6)	7664(3)	71(1)
C(76)	−2977(6)	3525(6)	7526(3)	54(1)

[a] Equivalent isotropic *U* defined as one-third of the trace of the orthogonalized U_{ij} tensor.

calculations were performed using the SHELXTL-PC package of programs.[18] Atomic scattering factors were taken from ref 19. Final atomic positional parameters for the non-hydrogen atoms for compounds **8a** and **9** are given in Tables VII and VIII, respectively.

Table VIII. Atomic Coordinates ($\times10^4$) and Equivalent Isotropic Displacement Parameters ($Å^2 \times 10^3$) for 9

name	*x*	*y*	*z*	*U*(eq)[a]
Mo	4381(1)	2843(2)	9647(2)	59(2)
Pt(1)	3860(1)	1486(1)	9201(1)	49(1)
Pt(2)	3061(1)	1380(1)	8177(1)	51(1)
W(1)	3872(1)	718(1)	7900(1)	47(1)
W(2)	2290(1)	2196(1)	8215(1)	58(1)
C(1)	5094(12)	2587(24)	9167(19)	45(7)
B(2)	5179(14)	2918(30)	9911(29)	56(7)
C(3)	4888(15)	2690(29)	10750(25)	73(7)
B(4)	4416(19)	2150(33)	10732(26)	71(7)
B(5)	4446(22)	1684(33)	9829(25)	83(7)
B(6)	4852(14)	1915(27)	9004(24)	41(7)
B(7)	4930(21)	1863(37)	11150(34)	91(7)
B(8)	4705(18)	1213(26)	10521(25)	65(7)
B(9)	5008(16)	1213(32)	9686(26)	71(7)
B(10)	5374(21)	1913(33)	9758(40)	95(7)
B(11)	5399(19)	2268(34)	10660(36)	85(7)
B(12)	5287(25)	1367(43)	10490(30)	128(7)
C(2)	5333(17)	2974(30)	8530(34)	125(7)
C(4)	4818(19)	3289(30)	11258(26)	111(7)
C(10)	4490(16)	3890(23)	9643(26)	85(7)
O(10)	4547(17)	4550(23)	9621(31)	162(7)
C(11)	3866(11)	3200(23)	10225(22)	47(7)
O(11)	3512(10)	3356(19)	10514(18)	86(7)
C(12)	4196(15)	2992(27)	8670(24)	80(7)
O(12)	4026(14)	3144(19)	8095(22)	117(7)
C(13)	3467(14)	1553(27)	10055(21)	71(7)
O(13)	3215(12)	1576(23)	10558(21)	117(7)
C(14)	4300(10)	1348(22)	8407(18)	41(7)
O(14)	4692(9)	1579(15)	8400(13)	54(6)
C(20)	3438(13)	606(24)	8726(23)	54(7)
C(21)	3244(12)	36(21)	9239(20)	37(6)
C(22)	3480(18)	−390(27)	9704(27)	86(7)
C(23)	3305(15)	−925(23)	10161(20)	56(7)
C(24)	2853(15)	−1061(23)	10124(23)	67(7)
C(25)	2562(18)	−658(27)	9621(26)	81(7)
C(26)	2766(14)	−52(29)	9221(22)	69(7)
C(27)	2622(13)	−1673(24)	10555(26)	68(7)
C(30)	3606(15)	1549(24)	7311(22)	57(7)
O(30)	3540(11)	1962(19)	6799(15)	75(7)
C(40)	2437(13)	1294(19)	7892(21)	38(7)
C(41)	2304(14)	625(20)	7417(25)	53(7)
C(42)	2516(14)	245(22)	6881(21)	49(7)
C(43)	2325(17)	−354(24)	6463(34)	101(7)
C(44)	1940(16)	−657(27)	6745(34)	123(7)
C(45)	1693(16)	−343(23)	7294(22)	60(7)
C(46)	1892(18)	249(31)	7588(40)	121(7)
C(47)	1734(27)	−1369(35)	6376(39)	181(7)
C(51)	3801(14)	−357(21)	7265(25)	67(7)
C(52)	4016(16)	111(25)	6812(25)	68(7)
C(53)	4469(17)	229(22)	7172(26)	65(7)
C(54)	4451(20)	−224(26)	7801(37)	117(7)
C(55)	4002(15)	−603(29)	7898(24)	83(7)
C(60)	2831(17)	2641(21)	8688(23)	57(7)
O(60)	3160(10)	3009(18)	8823(20)	85(7)
C(61)	2174(19)	1783(26)	9098(22)	85(7)
O(61)	2114(19)	1437(31)	9686(24)	162(7)
C(71)	1764(23)	3071(35)	8343(37)	166(7)
C(72)	2068(20)	3395(25)	7876(31)	107(7)
C(73)	2048(20)	2969(32)	7262(45)	163(7)
C(74)	1762(19)	2378(25)	7316(29)	94(7)
C(75)	1588(18)	2465(38)	8029(38)	125(7)

[a] Equivalent isotropic *U* defined as one-third of the trace of the orthogonalized U_{ij} tensor.

Acknowledgment. We thank the Robert A. Welch Foundation for support (Grants AA-1201 and 0668) and the University of Kent, Canterbury, U.K., for study leave for M.J.W.

Supplementary Material Available: Complete tables of bond lengths and bond angles, anisotropic thermal parameters, and hydrogen atom parameters for **8a** and **9** and an additional structure of **8a** (21 pages). Ordering information is given on any current masthead page.

OM930420F

---

(18) Siemens. SHELXTL-PC Siemens X-ray Instruments, Madison, WI, 1989.

(19) *International Tables for X-ray Crystallography*; Kynoch Press; Birmingham, U.K., 1974; Vol. 4.